HHS Public Access

Author manuscript

Gut. Author manuscript; available in PMC 2023 September 01.

Published in final edited form as:

Gut. 2022 September ; 71(9): 1790–1802. doi:10.1136/gutjnl-2021-324984.

RNA binding protein DDX5 directs tuft cell specification and function to regulate microbial repertoire and disease susceptibility in the intestine

Tianyun Long[1], **Nazia Abbasi**[1], **Juan E. Hernandez**[1], **Yuxin Li**[1], **Ibrahim M. Sayed**[2], **Shengyun Ma**[1], **Attilio Iemolo**[1], **Brian A. Yee**[1], **Gene W. Yeo**[1], **Francesca Telese**[1], **Pradipta Ghosh**[1,3,4], **Soumita Das**[2,4], **Wendy Jia Men Huang**[1,*]

[1]Department of Cellular and Molecular Medicine, University of California San Diego, La Jolla, CA

[2]Department of Pathology, University of California San Diego, La Jolla, CA

[3]Department of Medicine, University of California San Diego, La Jolla, CA

[4]HUMANOID Center of Research Excellence (CoRE), University of California San Diego, La Jolla, CA

Abstract

Objective—Tuft cells residing in the intestinal epithelium have diverse functions. In the small intestine, they provide protection against inflammation, combat against helminth and protist infections, and serve as entry portals for enteroviruses. In the colon, they had been implicated in tumorigenesis. Commitment of intestinal progenitor cells to the tuft cell lineage requires Rho GTPase Cell Division Cycle 42 (CDC42), a Rho GTPase that acts downstream of the Epidermal Growth Factor Receptor (EGFR) and Wnt signaling cascades, and the master transcription factor POU class 2 homeobox 3 (POU2F3). This study investigates how this pathway is regulated by the DEAD box containing RNA binding protein DDX5 *in vivo*.

Design—We assessed the role of DDX5 in tuft cell specification and function in control and epithelial cell-specific *Ddx5* knockout mice (DDX5$^{\Delta IEC}$) using transcriptomic approaches.

Results—DDX5$^{\Delta IEC}$ mice harbored a loss of intestinal tuft cell populations, modified microbial repertoire, and altered susceptibilities to ileal inflammation and colonic tumorigenesis. Mechanistically, DDX5 promotes CDC42 protein synthesis through a post-transcriptional mechanism to license tuft cell specification. Importantly, the DDX5-CDC42 axis is parallel but distinct from the known IL-13 circuit implicated in tuft cell hyperplasia, and both pathways augment *Pou2f3* expression in secretory lineage progenitors. In mature tuft cells, DDX5 not only

*Corresponding author; wjh003@ucsd.edu.

Author contributions

T.L. and N.A. designed and performed the mouse studies. T.L. and I.M.S. performed the small intestine and colon organoid assays. Y.L. performed the bioinformatics analyses on the RNAseq datasets. J.E.H performed the crypt and goblet cell analyses. B.A.Y. completed the eCLIPseq analyses. G.W.Y. directed the eCLIPseq studies and edited the manuscript. P.G. and S.D. directed the organoid studies and edited the manuscript. S.M. initiated the spatial transcriptomic studies and T.L. completed the studies with help from A.L.. F.T. provided resources for the spatial transcriptomic and organoid imaging studies. T.L. wrote the manuscript with input from W.J.M.H., N.A., and JE.H.

Conflict of Interest Statement

The authors declare no competing financial interests.

promotes integrin signaling and microbial responses, it also represses gene programs involved in membrane transport and lipid metabolism.

Conclusion—RNA binding protein DDX5 directs tuft cell specification and function to regulate microbial repertoire and disease susceptibility in the intestine.

Introduction

Intestinal epithelial cells (IEC) lining the gastrointestinal tract are essential for nutrient absorption and provide barrier protection for the host[1]. IECs are functionally heterogeneous. One subset called tuft cells is a major sensor of microbial challenges in the intestine. They express various unique surface molecules, including receptors that bind directly to noroviruses and receptors sensing microbial metabolites, including succinate[2–4]. During helminth and protist challenges, tuft cells secrete IL-25 to activate type 2 innate lymphoid cells (ILC2s). In a positive feedback circuit, activated ILC2s produces interleukin 13 (IL-13) to drive tuft cell hyperplasia and ensure robust microbial clearance[2 5–9]. Recent studies also revealed important roles of tuft cells in regulating inflammation and tumorigenesis in different intestine sections. In the ileum, reduction in tuft cell numbers is associated with elevated inflammation in the Crohn's disease (CD) patients[10]. Succinate activation of the tuft cell circuit is found be protective against T cell mediated ileitis in a mouse model[10]. In the colon, tuft cells and their unique expression of the pro-survival doublecortin-like kinase 1 (DCLK1) have been implicated in tumorigenesis[11 12].

IECs have diverse turnover rates ranging from 3–5 days for enterocytes to 3–6 weeks for Paneth cells[13 14]. They are replenished by progenitors originating from the intestinal stem cells (ISCs) residing in the crypt[13 15]. Progenitor differentiation to specific IEC lineages is influenced by local nutrient availability, microbial composition, and gradients of Epidermal Growth Factor (EGF), Wingless-related integration site (Wnt), Bone Morphogenetic Protein (BMP), as well as cytokines from the immune system[16–18]. Tuft cells in the small intestine and colon arise from the $SOX4^+$ and $ATOH1^+$ progenitors respectively[19–21]. Commitment to the tuft cell lineage requires the expression of the POU domain transcription factor, POU2F3[22]. A recent study has implicated Cell Division Cycle 42 (CDC42) in tuft cell biogenesis[23]. CDC42 is a ubiquitously expressed member of the Rho GTPase family. Upon activation by EGF and Wnt signaling cascades[24,23 25 26], CDC42 regulates actin cytoskeleton organization, polarity, proliferation, and migration[27 28]. Mutations in *Cdc42* have been linked to pediatric immunodeficiency[29] and severe developmental delay in patients with Takenouchi-Kosaki syndrome (TKS)[30 31]. Global knockout of *Cdc42* in mice is embryonic lethal[32]. Studies using mice where *Cdc42* is specifically knocked out in IECs showed that CDC42 is required for ISCs growth and survival. Biogenesis of tuft cell, but not other secretory IEC subsets, is CDC42 dependent[23]. However, little is known about how CDC42 contributes to tuft cell differentiation and upstream mechanisms involved in maintaining proper CDC42 expression in IECs. Here, we report that CDC42 promotes POU2F3 expression and tuft cell specification in the intestine, and this circuit is post-transcriptionally regulated by the RNA binding protein called DEAD-box helicase 5 (DDX5).

DDXs can directly bind to RNA substrates and utilize ATP hydrolysis energy to unwind RNA duplexes, facilitate RNA annealing, organize RNA-protein complex assembly,[33] and promote post-transcriptional processing[34]. They can also partner with transcription factors to regulate gene expression[35–38]. Our previous study revealed that DDX5 is the highest expressed member of the DDX family in the intestine epithelium[39]. Overexpression of DDX5 predicts worse relapse-free survival in CRC patients[40–42], and knockdown of DDX5 can significantly inhibited the growth of cancer cells in xenograft models[43 44]. We have recently reported that knocking out DDX5 in IECs protected against dextran sulfate sodium induced colitis as well as tumor formation in mice on a susceptible background[39]. Given the emerging role of intestinal tuft cells in regulating intestinal inflammation and tumorigenesis, we asked whether changes in tuft cell specification and/or function may underly the contribution of DDX5 to intestinal inflammation and tumorigenesis. Here, we report an essential role of DDX5 in maintaining CDC42-POU2F3 levels in secretory lineage progenitors to drive tuft cell specification in both small intestine and colon. In differentiated IECs, including tuft cells, DDX5 promotes anti-microbial gene programs to regulate microbial composition and disease susceptibilities in models of ileitis and tumorigenesis.

Methods

Mice

C57BL/6 wild-type (Stock No: 000664) and *Villin1Cre* (Stock No: 021504) mice were originally obtained from the Jackson Laboratory. Previously described $Ddx5^{flox}$ mice were obtained from Dr. Frances Fuller-Pace's laboratory[45]. Heterozygous mice were bred to yield 6–8 week-old $Ddx5^{+/+}$ $Villin1Cre^{+}$ (subsequently referred to as wild-type, WT^{IEC}) and $Ddx5^{fl/fl}$ $Villin1Cre^{+}$ (referred to as $DDX5^{\Delta IEC}$) cohoused littermates for experiments. For the tumor studies, Apc^{flox} mice were obtained from Dr. Eric Fearon's laboratory[46] to generate $Apc^{fl/+}$ $Ddx5^{+/+}$ $Villin1Cre^{+}$ and $Apc^{fl/+}$ $Ddx5^{fl/+}$ $Villin1Cre^{+}$ (referred as $APC^{\Delta IEC}$ $DDX5^{WT}$) and $Apc^{fl/+}$ $Ddx5^{fl/fl}$ $Villin1Cre^{+}$ ($APC^{\Delta IEC}$ $DDX5^{\Delta IEC}$) mice. Three (3) month old wildtype and mutant mice were given either 150 mM succinate (Alfa Aesar 41983–30) or control water (containing NaCl at 300 mM to match sodium molarity with succinate treatment) for 30 days. Colons were harvested from 120–130-day old mice to assess tumor burden. Tumor measurements were determined by double-blinded analyses using ImageJ. All animal studies were approved and followed the Institutional Animal Care and Use Guidelines of the University of California San Diego. Our vivarium at UC San Diego is kept under specific pathogen free (SPF) conditions. Regular serology and PCR tests are used to monitor and ensure the absence of EDIM, MHV, MPV, MVM, TMEV, fur mites and pinworms. MNoV is normally present in our vivarium, litters born to $MNoV^{+}$ parents naturally acquire the virus from their environment prior to weaning and were used for experiments between 8–12 weeks of age.

The spatial transcriptomic dataset described were performed on tissues obtained from female mice. DCLK1 immunohistochemistry experiments were performed on tissues from female mice. All other experiments reported in this study were obtained from both male and female mice in similar ratios.

Metronidazole treatment

For the antibiotic treatment studies, WT^{IEC} and $DDX5^{\Delta IEC}$ adult mice were treated with 1% sucrose alone or 1% sucrose containing 2.5 g/L of metronidazole in the drinking water for two weeks. New beddings were provided on day 7 to limit microbe reacquisition via the fecal-oral route. Mice were monitored and weighed 2–3 times per week and fecal/cecal material were collected to assess the level of protist and bacteria clearance. Pestle-homogenized fecal or cecal materials were digested at 75°C for 10min using the KAPA Express Extract kit (R&D). 1μL of the soluble fraction was used as template for qPCR quantitation.

Anti-CD3ε mediated model of ileitis

WT^{IEC} and $DDX5^{\Delta IEC}$ mice were given 300mM succinate-NaCl or equal molar of NaCl in drinking water for 2 weeks and subsequently i.p. injected 3 times with 15ug of anti-CD3ε per mouse every other day for 5 days[47].

Histology and immunohistochemistry

Tissues harvested from the ileum and colon were fixed overnight in 10% formalin (Research Products International) at room temperature. Paraffin-embedded tissues were sectioned into 5 μm slices for Periodic Acid-Schiff (PAS) or immunohistochemical (IHC) staining (see Supplementary Table 1 for antibody information). Briefly, paraffin sections were de-paraffinized and rehydrated with Tris-buffered saline (TBST, pH 7.8 with 0.1% Tween-20) washes between each step. Sections were blocked first against endogenous peroxidases (immersed for 30 minutes in 0.3% H_2O_2), and then blocked against endogenous biotin using unlabeled streptavidin (Jackson ImmunoResearch, 016-000-114) and excess free biotin. Antigen retrieval was induced by heating the slide twice for 5 minutes in 10 mM sodium citrate buffer pH 6.0 (Sigma-Aldrich), followed by 20 minutes of cooling. Finally, sections were blocked against non-specific hydrophobic interactions with 1% bovine serum albumin (BSA; Biotium) in TBST. Staining was then performed with either the negative control IgG antibody or anti-DCLK1 (1:1000) antibodies (Abcam) overnight in a humid chamber at 4°C. The next day, sections were washed with TBST and then sequentially overlaid with biotinylated goat anti-rabbit (Jackson ImmunoResearch, 111-065-045) at 1:500, followed by HRP-labeled Streptavidin (Jackson ImmunoResearch, 16-030-084) at 1:500. Substrate was then overlaid with 3-amino-9-ethylcarbazole from Vector labs following manufacturer directions for 30 minutes followed by nuclear counterstain with Mayer's hematoxylin. Images were acquired using the AT2 Aperio Scan Scope (UCSD Moores Cancer Center Histology Core). Three intestinal regions per tissue image were randomly selected for QuPath analysis. $DCLK^+$ tuft cells were determined by QuPath Positive Cell Detection[48] (minimum area = 10μm^2, maximum area = 400μm^2, intensity threshold = 0.4). $Mucin^+$ goblet cells were assessed similarly (minimum area = 40μm^2, maximum area = 800μm^2, intensity threshold = 0.6). The average score from three regions examined in each tissue were included in the final graph.

Electron microscopy

Cardiac perfusion was performed using 5mL Ringer's solution (Fisher Scientific, Cat. #50-980-246), followed by 5ml of fixation buffer containing 2% Paraformaldehyde/2.5% Glutaraldehyde in 0.1M Sodium Cacodylate buffer solution (BIOTREND, Cat.# 15960–01). Intestinal tissues were harvested and kept in the fixation buffer in room temperature for 3 additional hours. Fixed tissues were processed and imaged on JEOL 1400 plus at the UC San Diego Electron Microscopy Core Facility.

Intestinal epithelial and lamina propria lymphocyte harvest

Steady-state intestinal epithelial and lamina propria lymphocytes were harvested as previously described[49]. To isolate IECs, intestinal tissues were first incubated in 5 mM EDTA (Invitrogen) in HBSS (Gibco) containing 1 mM DTT (Invitrogen) for 20 minutes at 37°C with 200rpm agitation, and then incubated in a second wash of 5 mM EDTA in HBSS without DTT for another 20 minutes at 37°C with agitation. Single-cell suspensions released into the EDTA solutions were pooled and confirmed to contain over 85% $EpCAM^+$ IECs as reported previously[39]. For the lamina propria, IEC-depleted tissues from post-EDTA washes were digested in a HBSS solution containing 10% Fetal Bovine Serum (Peak Serum), 1.0 mg/ml Collagenase D (Roche), 100 μg/ml DNase I (Sigma-Aldrich), and 50 U/ml dispase (Worthington Biochemical Corporation) at 37°C for 30–45 minutes. Lamina propria mononuclear lymphocytes were purified from the interphase of a 40:80% Percoll™ (Cytiva; formerly GE Healthcare Life Sciences) gradient.

Intestinal crypt isolation and organoid culture

Small intestinal and colonic crypts were isolated according to the manufacturer's recommendation (STEMCELL, technical bulletin #28223). Briefly, 20cm of small intestine proximal to the stomach were harvested from 6–8 week-old WT^{IEC} and $DDX5^{\Delta IEC}$ littermates and cut into 2mm pieces. After 20 washes in cold PBS, tissues were resuspended in 25mL room temperature Gentle Cell Dissociation Reagent (STEMCELL, #07174) and incubated at room temperature for 15 minutes on a rocking platform at 20 rpm. The pellets enriched with intestinal crypts were resuspended in cold PBS containing 0.1% BSA. Isolated colonic crypts were embedded in Corning® Matrigel® Matrix (Corning™ 356231) and seeded onto pre-warmed, non-treated 24-well plates (CytoOne® by StarLab) and overlaid with conditioned media (STEMCELL, #6005) as described previously[50]. Organoids were treated with recombinant mouse IL-13 (BioLegend, 20ng/ml), NaCl (Sigma, 15μM), DMSO (Sigma), or ML141 (Cayman Chemical, 10μM). Organoid pictures were imaged using a Keyence bz-x800 microscope at 20X magnification with image stacks capturing the entire organoid volume.

Retroviral transduction

Authenticated Platinum-E (Plat-E) cells purchased from ATCC were grown in DMEM medium (Gibco) containing 1% L-glutamine (Gibco) and 10% fetal bovine serum (FBS; Thermo Fisher Scientific). Plat-E cells were transfected with MSCV constructs using TransIT®-LT1 Transfection Reagent (Mirus) following the manufacturer's instructions. Virus-containing supernatant collected three days after the infection was concentrated using

Retro-X concentrator (Takarabio). Virus was resuspended in organoid medium containing 8μg/ml polybrene. Dissociated organoids were resuspended in virus-containing medium for spin inoculation (600g at 32°C for 60 min) followed by a six-hour incubation at 37°C. Transduced cells were collected and seeded in Matrigel. Media was changed every 2–3 days. Organoids were analyzed by flow cytometry and/or RT-qPCR 7 days post-transduction.

Flow cytometry analysis

For analysis of tuft cells in intestinal epithelium and organoids, cells were surface stained with LIVE/DEAD Fixable Cell stain (ThermoFisher, L34957), and fluorescent conjugated antibodies against EpCAM, CD24, CD45, Siglec-F, and CD90.1 (see Supplementary Table 1 for detailed information, 1:400 in PBS) for 30 minutes. For intracellular staining of CDC42, cells were fixed/permeabilized (ThermoFisher Cat: 00-5521-00), incubated with the anti-CDC42 antibody (ThermoFisher, 1:50) for 1h in room temperature, followed by the anti-rabbit IgG (H+L) Cross-Adsorbed Secondary Antibody (Invitrogen, 1:400) for 1h in 4°C. IECs were defined as live $CD4^{-}CD8^{-}Epcam^{+}CD45^{low}$. Successfully transduced organoid cells were defined as $CD90.1^{+}$. Proportion (%) of IECs in the tuft cell lineage were defined as $Siglec\text{-}F^{+}CD24^{+}$ as previously described[51]. Flow cytometry data was analyzed with FlowJo (version 10.8.1).

Western blot

Cells were lysed in a 25 mM Tris pH 8.0 (G-Bioscience, 100 mM NaCl (G-Bioscience), 0.5% NP40 (G-Bioscience) solution with protease inhibitor (Life technologies) for 30 min on ice. Samples were spun down at 14,000 × *g* for 15 min, and soluble protein lysates were harvested. 30–50μg protein were loaded in each lane of a SDS-PAGE gel. Blots were blocked in Odyssey Blocking buffer (Li-CoR Biosciences) and probed for CDC42. Following incubation with IRDye secondary antibody (Li-CoR® Biosciences), infrared signals on each blot were collected on the Li-CoR Odyssey CLX. The primary antibodies used in this study are listed in Supplementary Table 1.

cDNA synthesis and qPCR

Total RNA was extracted with the RNeasy Plus kit (QIAGEN) and reverse transcribed using iScript™ Select cDNA Synthesis Kit (Bio-Rad). Real time RT-PCR was performed using iTaq™ Universal SYBR® Green Supermix (Bio-Rad). For primary IECs, results were normalized to mouse *Gapdh*. For organoid studies, results were normalized to β-actin. Primers were designed using Primer-BLAST to span across splice junctions, resulting in PCR amplicons that span at least one intron. Primer sequences are listed in Supplementary Table 2.

RNA-seq analysis

Intestinal epithelial cell transcriptomes from WT^{IEC} and $DDX5^{\Delta IEC}$ littermates were previously reported[39]. Gene set enrichment analysis was carried out using the pre-ranked mode of the Gene Set Enrichment Analysis (GSEA) software with default settings[52]. The gene list from DEseq2 was ranked by calculating a rank score of each gene as $-\mathrm{Log}_{10}(p\text{-}value) \times \mathrm{sign}\,(\mathrm{Log}_2\ \mathrm{Fold\ Change})$, in which Fold Change is the fold change

of gene expression in DDX5 $^{\Delta IEC}$ over that found in WT^{IEC}. *De novo* motif enrichment in the promoter regions of differentially expressed genes (log_2 fold change cutoffs of ≥ 0.5 or ≤−0.5 and *p*-values <0.05) was performed using the HOMER (v4.10) "findMotifs.pl" command line with the following parameters: "-nogo -start −1000 -end 500"[53]. All other promoters of genes expressed in those particular cells were used as background. The top 5 motifs ranked by the lowest *p*-value that were found in at least 3% of the differentially expressed "Target" genes were illustrated. The tumor transcriptomic sequencing data reported in this paper is available on GEO (GSE146014, reviewer access token: gbahcsuozruptyf).

For metatranscriptomic analysis of ileal associated microbial populations, reads from the $DDX5^{\Delta IEC}$ and WT^{IEC} IEC RNAseq dataset that were not mapped to the mouse genome were assigned with taxonomic labels using Kraken v1. The standard Kraken database encompassing annotated bacterial, archaeal, and viral genomes was used for classification of sequences with the command: "kraken --classified-out /path/to/classified_fq --unclassified-out /path/to/unclassified.fq --db $DBNAME --paired --fastq-input pair1.fa pair2.fa > /path/to/results". A Kraken report was generated with the the command: "kraken-report --$DBNAME kraken.output"[54]. Differential microbial counts were assessed by DEseq2 cut off of $p<0.05$ with the Wald test and Log2 fold change ($DDX5^{\Delta IEC}/WT^{IEC}$)>1.5 or <−1.5.

Spatial transcriptomics

Female mouse ileum samples were coiled into "Swiss rolls" and frozen immediately with chilled isopentane. The frozen tissues were embedded in Optimal Cutting Temperature (OCT) compound and cut in a pre-cooled cryostat at 20mM thickness onto two 6.5mm × 6.5mm capture areas with 5000 oligo-barcoded spots. Frozen tissue was tested for RNA quality with RIN > 7.0 (Tapestation). Slides were fixed, H&E stained, and imaged on Keyence (bz-x800) at 20x magnification. Tissues were permeabilized for 24 minutes. Reverse transcription and second strand synthesis were then performed on RNAs extracted from each tissue. cDNAs were quantified by qRT-PCR using Powerup SyBr Green master mix and the Bio-Rad system. The library integrity was confirmed by the Agilent TapeStation. Pooled libraries were sequenced on NovaSeq S4 (Illumina) using 150 base-pair paired-end dual-indexed configuration. Each sample was sequenced to a depth of 100 million. Spaceranger software (version 3.1.0) from 10X Genomics was used to process, align and summarize unique molecular identifier (UMI) counts against the mm10 human reference genome. Loupe Browser (version 5.0) was used for differential gene expression analysis and generation of visuals. The spatial transcriptomic sequencing data reported in this paper is available on GEO (GSE184564, reviewer access token: obaruukivrmpxad).

Ribosome pull-down assay

Small intestine IECs were lysed in polysome extraction buffer (10 mM HEPES, pH 7.4, 150 mM KCl, 5 mM MgCl2, 1% NP40, 2 mM dithiothreitol, 80 U/ml RNaseOUT, 100 μg/ml cycloheximide, and protease inhibitors). Cell extracts were subject to anti ribosome IP_overnight with 2 μg anti-RPL10A antibodies (Abcam) as described previously[39]. Level

of RPL10A associated transcripts in pull-down was calculated as fraction of input for each sample.

Statistical analysis

All values are presented as mean ± standard deviation (SD). Significant differences were evaluated using GraphPad Prism 8 software (GraphPad). The Student's *t*-test was used to determine significant differences between two groups with normal distribution. A two-tailed *p*-value of <0.05 was considered statistically significant in all experiments.

Results

DDX5 regulates tuft cell populations in the murine small intestine and colon

In our previous report, we showed that DDX5 is highly expressed in the intestinal epithelium and regulates intestinal inflammation. However, the exact mechanism remained to be elucidated. In a recent studies activation of the tuft cell circuit is also linked to intestinal inflammation[10]. Therefore, we asked whether DDX5 may regulate intestinal inflammation at least in part by contributing to the differentiation and function of tuft cells and/or other IEC subsets. To address this question, we performed lineage-specific Gene Set Enrichment Analysis (GSEA) on our previously reported transcriptomes of steady-state IECs obtained from two matched pairs of WT^{IEC} and $DDX5^{\Delta IEC}$ male littermates[39]. A loss of the tuft cell signature was found in both the small intestinal and colonic epithelia of $DDX5^{\Delta IEC}$ mice (Figure 1A–B and Supplementary Figure 1A). IECs from independent pairs of male and female WT^{IEC} and $DDX5^{\Delta IEC}$ littermates were used to confirm significant reductions in the expressions of two tuft cell-specific transcripts, *Pou2f3 and Dclk1*. In contrast, comparable expressions of select transcripts previously shown to be enriched in other IEC subsets, including *Maf* (enteroendocrine cells), *Muc2* (goblet cells), *Lyz1* (Paneth cells), *Lgr5* and *Ki67* (ISCs), were found in control and $DDX5^{\Delta IEC}$ mice (Supplementary Figure 1B). These results suggest that DDX5 may have a unique role in regulating tuft cell differentiation and/or function in the intestine.

Next, we investigated whether the loss of tuft cell gene signature in $DDX5^{\Delta IEC}$ IECs may be due to a loss of the intestinal tuft cell population. Indeed, immunohistochemistry analysis revealed a significant reduction of $DCLK1^{+}$ tuft cells in the $DDX5^{\Delta IEC}$ small intestine and colon (Figure 1C–D, workflow described in Supplementary Figure 2A). In contrast, Periodic acid-Schiff staining (PAS) of the small intestine and colon sections from control and $DDX5^{\Delta IEC}$ mice showed comparable crypt density and goblet cell numbers (Supplementary Figure 2B–D). Consistent with the histology results, flow cytometry analysis of the small intestine and colonic IECs (defined as $CD45^{-}EpCAM^{+}$) also confirmed a significant reduction of tuft cells (defined as $Siglec\text{-}F^{+}CD24^{+}$, similar to a previous report[51]) in the $DDX5^{\Delta IEC}$ IECs from male and female mice (Figure 1E, gating strategy detailed in Supplementary Figure 3A). These results demonstrate that DDX5 promotes tuft cell biogenesis in the murine small intestine and colon. In two human colonic IEC transcriptomic datasets previously reported[55 56], elevated *DCLK1* expression was also associated with higher *DDX5* expression (Figure 1F), suggesting regulation of the tuft cell gene program by DDX5 is likely evolutionarily conserved.

Impaired expression of the tuft cell commitment factor, *Pou2f3*, in DDX5$^{\Delta IEC}$ IEC secretory lineage progenitors

In the small intestine, ATOH1 and SOX4 expressing IECs are progenitors of the secretory lineages, including tuft cells, goblet cells, Paneth cells, and enteroendocrine cells[20 57 58]. Next, we asked whether DDX5 contribute to the generation of these progenitor populations and/or their ability to express factors required for the generation of each secretory lineage, including *Pou2f3*-*Gfi1b* for tuft cells, *Spdef* for Goblet cells, *Sox9* for Paneth cells, and *Neurod1* for enteroendocrine cells. Spatial transcriptomics (10X Visium) analysis of ileal sections revealed similar number of *Atoh1*^{high} and *Sox4*^{high} spots were present in the WT^{IEC} and DDX5$^{\Delta IEC}$ tissues (Figure 2A). As expected, *Pou2f3* transcripts were more abundantly found in *Sox4*^{hi} spots than *Atoh1*^{hi} spots in the wildtype ileum. However, its expression was greatly reduced in both *Sox4*^{high} and *Atoh1*^{hi} spots from the DDX5$^{\Delta IEC}$ ileum (Figure 2B). In contrast, *Atoh1*^{high} spots from the DDX5$^{\Delta IEC}$ ileum showed higher levels of *Neurod1*, but similar levels of *Gfi1*, *Spdef*, and *Sox9* compared to *Atoh1*^{high} spots from WT^{IEC} ileum (Supplementary Figure 4A). Similar differential gene expression analysis on Lgr5^{hi} spots, but revealed only a relatively minor footprint of DDX5 in the ISCs (Supplementary Figure 4B and Supplementary Table 3), consistent with our earlier observation from our bulk IEC analysis (Supplementary Figure 1B). These results suggest that DDX5 may regulate tuft cell biogenesis by promoting *Pou2f3* expression in the secretory lineage progenitors.

Consistent with findings from the spatial transcriptomic studies, small intestine crypts enriched with ISC and progenitors isolated from DDX5$^{\Delta IEC}$ mice had lower *Pou2f3* mRNA abundance compared to those found in crypts obtained from their WT^{IEC} littermates (Supplementary Figure 4C). In addition, DDX5$^{\Delta IEC}$ small intestinal crypts cultured *ex vivo* over 4–7 passages in the presence of the Wnt pathway agonist R-spondin (Rspo), epidermal growth factor (EGF), the BMP inhibitor Noggin (as previously described[16]), penicillin, streptomycin, and gentamicin developed into organoids and maintained lower *Pou2f3* expression compared to those derived from WT^{IEC} mice (Figure 2C–D). Similar observations were found in DDX5$^{\Delta IEC}$ colonic organoids (Figure 2E). No significant change in organoid viability and size were found between cultures obtained from control or DDX5$^{\Delta IEC}$ crypts (Supplementary Figure 5A). Furthermore, tuft cell-specific genes harboring a promoter POU2F motif had the greatest loss in the expression in the DDX5$^{\Delta IEC}$ tissue (Figure 2F–G). Together, these results demonstrate an epithelial cell-intrinsic role of DDX5 in maintaining *Pou2f3* expression *in vivo* and *ex vivo*.

DDX5 is dispensable for IL-13 driven tuft cell hyperplasia

Differentiation of IEC subsets, including tuft cells, is heavily influenced by the local microbial composition and immune cytokine profiles. In the presence of protozoan *Trichomonas muris*, for example, the small intestinal tuft cell population expands rapidly in an IL-13-dependent manner[3 4]. Therefore, we asked whether the loss of tuft cell numbers in the DDX5$^{\Delta IEC}$ intestine may be explained by a reduction in local IL-13 level, difference in *Trichomonas* abundance, and/or expressions of IL-13 receptors in the ISC and progenitors. At the RNA level, we found a similar abundance of transcripts encoding *Il13* expressed by immune cells in the lamina propria of cohoused WT^{IEC} and DDX5$^{\Delta IEC}$ littermates (Supplementary Figure 6A). Furthermore, cohoused WT^{IEC} and DDX5$^{\Delta IEC}$

littermates acquired similar levels of *Trichomonas* species from their parents prior to weaning (Supplementary Figure 6B).

To assess whether the *Trichomonas* species present in our mouse colony were implicated in the tuft cell specification, we treated cohoused WT^{IEC} and $DDX5^{\Delta IEC}$ littermates with metronidazole in drinking water for 14 days to deplete majority of the *Trichomonas* species together with other metronidazole sensitive bacterial species (Supplementary Figure 6B). Interestingly, WT^{IEC} mice treated with metronidazole had no significant change in the proportion of tuft cells in the small intestine and colon as measured by flow cytometry (defined as Siglec-$F^{+}CD24^{+}$). Likewise, the proportion of tuft cells and epithelial *Pou2f3* transcript levels in the metronidazole-treated $DDX5^{\Delta IEC}$ mice remained lower than levels found in WT^{IEC} mice under similar treatment (Supplementary Figure 6C). These results suggest that the metronidazole-sensitive *Trichomonas* and bacteria species present in our mouse colony were not involved in the establishment of tuft cell in the WT^{IEC} and $DDX5^{\Delta IEC}$ mice. It remained to be investigated whether specific metronidazole-insensitive microbe(s) and/or metabolites present in our colony contribute to the DDX5-dependent generation of tuft cell we observed.

Furthermore, we found no defect in the ability of $DDX5^{\Delta IEC}$ ISC and secretory lineage progenitors to express genes encoding receptors for IL-13 (Supplementary Figure 7A). Therefore, we hypothesized that DDX5 is likely dispensable for tuft cell hyperplasia in response to IL-13. To test this possibility, WT^{IEC} and $DDX5^{\Delta IEC}$ small intestinal and colonic organoids were treated with recombinant IL-13 for three days. At the RNA level, both WT^{IEC} and $DDX5^{\Delta IEC}$ organoids upregulated *Pou2f3* to a similar extent, resulting in a ≥2 fold increase in tuft cell numbers compared to vehicle-treated organoids (Supplementary Figure 7B–D). Together, these results suggest that DDX5 is dispensable for type 2 immune cytokine-driven tuft cell hyperplasia.

DDX5 promotes *Cdc42* translation to induce tuft cell biogenesis

Next, we asked whether DDX5 promotes *Pou2f3* expression and drives tuft cell biogenesis by directly binding to *Pou2f3* mRNA and/or transcripts encoding its upstream regulators. To this end, we examined the DDX5-associated RNA interactome identified by the enhanced cross-linked immunoprecipitation (eCLIPseq) experiment on IECs derived from the steady-state WT small intestine[39]. To our surprise, we did not identify any DDX5 footprint on the *Pou2f3* transcript, suggesting that DDX5 likely regulate *Pou2f3* expression indirectly. Of the eleven known molecules previously implicated in *Pou2f3* expression and tuft cell biogenesis (*Gfi1b, Mtor, Rptor, Stat6, Ogt, Tas1r3, Sox4, Hes1, Dll1, Atoh1*, and *Cdc42*), only the *Cdc42* transcripts were bound by DDX5 (Figure 3A). CDC42 is a GTP-binding protein previously implicated in ISC survival, growth, as well as tuft cell biogenesis[23]. In the absence of DDX5, IECs had reduced CDC42 protein abundance (Figure 3B). Spatial transcriptomics analysis revealed that *Cdc42* is ubiquitously expressed across all IEC subsets, and most abundantly found in $Lgr5^{hi}$ ISCs and $Sox4^{hi}$ progenitors (Figure 3C). Murine retrovirus carrying a CDC42 (isoform 1, V1) expression construct partially rescued CDC42 protein levels in $DDX5^{\Delta IEC}$ small intestinal organoids (Supplementary figure 8A–B) and restored the Siglec-$F^{+}CD24^{+}$ tuft cell population to levels found in WT^{IEC} cultures

(Figure 3D–E). These results demonstrate that DDX5 promotes tuft cell biogenesis by regulating CDC42.

EGF and R-spondin in the organoid culture media engage EGFR and Wnt signaling pathways known to drive CDC42 activity. At the RNA level, small intestinal *Sox4*^{hi} progenitors abundantly expressed *Egfr*, *Fzd2, and Lrp5* (Figure 3F). Therefore, we asked whether CDC42 GTPase activity may be implicated in the generation of tuft cells in the organoid culture system. Consistent with this possibility, DDX5$^{\Delta IEC}$ small intestinal organoids transduced with the dominant negative CDC42^{T17N} or CDC42^{G12V} expression constructs failed to restore the Siglec-F^{+}CD24^{+} tuft cell population (Figure 3D), suggesting that the GTPase activity of CDC42 is required for DDX5-mediated tuft cell biogenesis. To bypass the essential function of CDC42 in ISC reported previously[23 59], established WT organoids were passaged, seeded on fresh Matrigel, and allowed to differentiate normally for 48hrs and then subjected to CDC42 inhibition by ML141. In this assay, acute ML141 treatment did not result in measurable difference in organoid survival or growth (Supplementary Figure 9A). We also did not detect significant change in the abundance of *Klf4*, *Lyz1*, and *Lgr5* transcripts in ML141 treated organoids (Supplementary Figure 9B). However, *Pou2f3* expression was significantly diminished in WT organoids transiently treated with ML141 for 24hrs (Figure 3G). Intriguingly, ML141 treated wildtype small intestinal and colonic organoids remained responsive to IL-13 by expanding their tuft cell population to a similar extent as control treated cultures (Supplementary Figure 9C–D). Together, these results confirm that the DDX5-CDC42 axis is dispensable for IL-13-induced tuft cell expansion *ex vivo*.

Mechanistically, DDX5 did not alter IEC *Cdc42* transcript abundance (Figure 3HI). Ribosome capture assay revealed that optimal translation machinery engagement on *Cdc42* mRNA transcripts in small intestinal IECs was DDX5-dependent (Figure 3J). Intriguingly, retrovirus carrying wildtype DDX5 or the helicase dead DDX5^{DEAD}, expression constructs were able to rescue the Siglec-F^{+}CD24^{+} tuft cell population in DDX5$^{\Delta IEC}$ small intestinal organoids to levels found in WT^{IEC} cultures (Figure 3D). This suggests that DDX5 helicase activity is dispensable for promoting *Cdc42* ribosomal engagement. Together, results from our genetic, genomic, and pharmacological experiments demonstrate that epithelial DDX5 binds *Cdc42* transcripts and promotes CDC42 protein translation in a helicase activity-independent manner to control tuft cell biogenesis.

DDX5 negatively regulates tuft cell lipid and protein metabolic programs

Despite a significant loss of tuft cells in the DDX5$^{\Delta IEC}$ intestine, both immunohistochemistry and flow cytometry analyses demonstrated a small population of tuft cells can be generated in the absence of DDX5 (Figure 1C–E). Next, we tested whether DDX5$^{\Delta IEC}$ tuft cells may be morphological and/or functional distinct from those with intact DDX5 expression. Electron microscopy revealed similar brush-like microvilli structures characteristic of elongated tuft cells in both WT^{IEC} and DDX5$^{\Delta IEC}$ small intestine (Figure 4A), suggesting that DDX5 does not influence tuft cell morphology.

Previous reports clustered the small intestinal tuft cells into two main subsets: one having higher expression of genes related to neuronal development (type 1), and the other (type

2) enriched with immune-related genes, such as the Protein Tyrosine Phosphatase Receptor Type C gene encoding the pan-immune cell marker CD45[1 60]. Of the few DDX5$^{\Delta IEC}$ tuft cells present in the small intestine, their proportion of CD45 low- and mid-subpopulations were similar to those found among WT^{IEC} tuft cells (Supplementary Figure 10A). GSEA of the small intestinal IEC transcriptomes[39] also confirmed that both type 1 and 2 programs were significantly impaired in the DDX5$^{\Delta IEC}$ epithelium (Supplementary Figure 10B).

To fully elucidate IEC subset-specific DDX5-dependent gene programs, we performed differential gene analysis on the spatial transcriptomic datasets obtained from the WT^{IEC} and DDX5$^{\Delta IEC}$ small intestinal sections discussed in Figure 2A. We uncovered 17.5% of the DDX5-induced transcripts and 3.8% of the DDX5-repressed genes were shared among tuft, enteroendocrine, goblet, and Paneth cells (Supplementary Figure 11A–B and Supplementary Table 4). The numbers of DDX5-regulated genes in goblet and enteroendocrine cells is lower than those found in tuft and Paneth cells. Notably, DDX5$^{\Delta IEC}$ small intestinal tuft cells had reduced expression of genes involved in microbial responses (Figure 4B–D), including a loss of *Cd300lf* transcripts encoding a surface molecule used by the Murine norovirus (MNoV) as a key docking site for host entry[2] (Supplementary Figure 12A). As a result, DDX5$^{\Delta IEC}$ mice raised by MNoV^{+} parents had significantly fewer MNoV transcripts in their small intestinal epithelium compared to their cohoused wildtype littermates (Supplementary Figure 12A). In addition, meta-transcriptomic analyses of the WT^{IEC} and DDX5$^{\Delta IEC}$ intestinal epithelium transcriptomes revealed significantly lower mucosal-associated reads mapping to viral and bacterial genomes from the DDX5$^{\Delta IEC}$ small intestine and colon, respectively (Supplementary Figure 12B–C). In particular, species of *Helicobacters* and *Prevotella* were significantly reduced in the DDX5$^{\Delta IEC}$ colon (Supplementary Figure 12D and Supplementary Table 5).

While none of the DDX5-dependent genes involved in microbial responses harbor a DDX5 eCLIPseq footprint, ten of the genes involved in transmembrane transport and protein and lipid metabolism that were upregulated in DDX5$^{\Delta IEC}$ tuft cells were direct targets of DDX5 (indicated with a blue star on Figure 4E). These results reveal a novel role of DDX5 as a repressor of transmembrane transport and protein and lipid metabolic programs in tuft cells of the small intestine. Together, these results extend the role of DDX5 in shaping IEC subset gene programs and modulating the microbial community in the intestine.

Succinate-induced tuft cell hyperplasia protects against ileitis and restores colon tumorigenic potential in DDX5$^{\Delta IEC}$ mice

Small intestinal tuft cells have been recently reported to provide protection against T-lymphocyte mediated ileitis upon anti-CD3ε challenge[10]. Therefore, we hypothesized that the reduced tuft cell numbers in the small intestine of DDX5$^{\Delta IEC}$ mice may result in enhanced susceptibility to ileitis. Consistent with our hypothesis, 50% of the DDX5$^{\Delta IEC}$ mice challenged in this model succumbed to the disease by day 18 (Figure 5A). Of the ones that survived, mononuclear immune cells from their ileal lamina propria had elevated transcripts encoding the inflammatory cytokine TNF (Figure 5B). Pre-administration of succinate, a microbial-derived metabolite known to promote tuft cell hyperplasia in an IL-13 dependent manner[4 6], in drinking water was able to partially restore *Dclk1* expression in the

small intestine epithelium of DDX5$^{\Delta IEC}$ mice (Figure 5C), similar to previous reports[3 10], dampened *Tnf* expression, and significantly protected them against mortality from the anti-CD3ε challenge (Figure 5A–B).

In the colon, multiple IEC subsets, including DCLK1^{+} tuft cells, have been reported to harbor tumorigenic potential[11 12]. We recently reported that DDX5$^{\Delta IEC}$ mice on the intestinal tumor-susceptible *Apc*$^{\Delta IEC}$ background[46] harbored fewer intestinal tumors[39]. Transcriptomic analysis of control and DDX5 deficient tumors revealed pathways as well as a subset of DDX5-dependent genes that were similarly regulated in tuft cells (Supplementary Figure 13A–C and Supplementary Table 6). Therefore, we tested whether succinate supplementation can also promote colonic tuft cell programs, including *Dclk1* expression, and restore the tumorigenic potential of the APC$^{\Delta IEC}$DDX5$^{\Delta IEC}$ mice. Immunohistochemistry analysis confirmed partial restoration of the DCLK1^{+} population in succinate treated DDX5$^{\Delta IEC}$ mice (Figure 5D). In the tumor susceptible background APC$^{\Delta IEC}$, succinate treated DDX5$^{\Delta IEC}$ mice had higher colonic tumor counts than those treated with vehicle control alone (Figure 5E). Altogether, these results highlight the critical roles of epithelial DDX5 in protecting against ileal inflammation yet contributing to colonic tumorigenesis (modeled in Figure 5F).

Discussion

Tuft cells in the small intestine and colon arise from the SOX4^{+} and ATOH1^{+} progenitors respectively[19–21]. Commitment to the tuft cell lineage requires the expression of the POU domain transcription factor, POU2F3[22]. Induction of *Pou2f3* is best characterized in response to IL-13 and IL-4 stimulation during helminth and protist challenges[2 5–9]. However, the molecular mechanisms that control *Pou2f3* expression in the absence of IL-13 and IL-4 stimulation remain elusive. Here, we report that CDC42 and its GTPase activity is essential for *Pou2f3* expression. Consistent with our findings, epithelial specific knockout of CDC42 resulted in a loss of intestinal tuft cells, but no change to other secretory IEC subsets[23]. In the small intestine, we show that *Cdc42* is the abundantly expressed in ISCs and secretory lineage progenitor cells. Optimal translation of the *Cdc42* transcript rely on the RNA binding protein DDX5 in a helicase-activity independent manner. Knocking out DDX5 specifically in IECs results in reduced CDC42 protein abundance and loss of tuft cell populations in both the small intestine and colon. *Ex vivo*, retroviral expression of wildtype CDC42 rescued the tuft cell biogenesis defect in small intestinal DDX5$^{\Delta IEC}$ organoids.

Surprisingly, the DDX5-CDC42 axis is dispensable for tuft cell hyperplasia in response to IL-13. WT organoids cells treated with the CDC42 inhibitor and DDX5$^{\Delta IEC}$ organoids remain capable of responding to IL-13, upregulating *Pou2f3* expression, and inducing tuft cell expansion. Future studies will be needed to investigate whether these parallel DDX5-CDC42 and IL-13-induced pathways recruit shared or distinct transcription factors and/or machineries to drive *Pou2f3* expression in the secretory lineage progenitors. Compared to the secretory lineage progenitors, DDX5 has a limited transcription footprint on ISCs. We also did not find abnormalities in growth and survival in the DDX5$^{\Delta IEC}$ crypts containing ISCs and progenitors, unlike those observed in cells from the CDC42$^{\Delta IEC}$ mice[23]. We speculate that this likely suggest that the remaining CDC42 levels in the DDX5$^{\Delta IEC}$

epithelium is sufficient to maintain ISC growth and survival and/or CDC42 expression in ISC may be DDX5-independent. Future studies that genetically ablate *Ddx5* in specific IEC progenitor and/or IEC subsets will be needed to more definitively address whether the contribution of DDX5 to tuft cell differentiation and function may be cell-autonomous and/or indirect.

In the small intestine, tuft cells protect against ileal inflammation in a mouse model and a loss of tuft cells is identified in Crohn's disease patients[10]. As expected, DDX5$^{\Delta IEC}$ mice with reduced intestine tuft cell biogenesis were more susceptible to disease in a model of ileitis. Administration of succinate partially restored tuft cell numbers in DDX5$^{\Delta IEC}$ mice and allowed for greater resilience during ileitis. Compared to the small intestine, the colon epithelium harbored fewer tuft cells and their physiologic and pathologic functions are not well understood. Results from this study suggest that the DDX5-CDC42 axis is also implicated in colonic tuft cell biogenesis. In contrast to the anti-inflammatory role of DDX5 in the small intestine IECs, we previously reported that DDX5 in the colonic IECs promotes inflammation in a DSS-induced model of colitis[39]. Regional specific roles of DDX5 in intestine inflammation may be related to distinct microbe-host interactions and/or distinct gene programs regulated by DDX5 in colonic IECs. Future single-cell transcriptomic studies will be needed to fully elucidate the mechanisms underlying these specificities. Development of additional IEC-subset specific knockout models will be needed for definitively attributing specific DDX5 regulated programs to the various phenotypes observed here.

In summary, this study uncovered an epithelial cell intrinsic pathway involving the RNA binding protein DDX5 and its ability to regulate the CDC42-POU2F3 axis critical for tuft cell biogenesis that is parallel but distinct from the IL-13 induced hyperplasia responses and can serve as new molecular targets for the restoration of mucosal homeostasis in disease settings.

Supplementary Material

Refer to Web version on PubMed Central for supplementary material.

Acknowledgements

We thank Frances Fuller-Pace for sharing the DDX5 conditional mutant mice previously described[45]. We thank Jakob von Moltke at the University of Washington, Seattle, Elina Zuniga, Stephen Hedrick, and Karen Sykes at the University of California, San Diego, for critical reading of our manuscript.

T.L., N.A., Y.L., J.E.H., and W.J.M.H. are partially funded by the Edward Mallinckrodt, Jr. Foundation and the National Institutes of Health (R01-GM124494 to W.J.M.H). P.G and S.D. were funded by the National Institutes for Health (NIH) (R01-AI141630 to P.G., DK107585 to S.D. and UG3TR003355, UG3TR002968 and R01-AI55696 to P.G. and S.D.). P.G. and S.D. were also supported by the Leona M. and Harry B. Helmsley Charitable Trust. RNAseq was conducted at the IGM Genomics Center, University of California San Diego. We thank the UC San Diego Electron Microscopy Core, HUMANOID Core, and the Moores Cancer Center Histology Core supported by the National Cancer Institute (CCSG P30-CA23100).

References

1. Haber AL, Biton M, Rogel N, et al. A single-cell survey of the small intestinal epithelium. Nature 2017;551(7680):333–39. doi: 10.1038/nature24489 [published Online First: 2017/11/17] [PubMed: 29144463]
2. Wilen CB, Lee S, Hsieh LL, et al. Tropism for tuft cells determines immune promotion of norovirus pathogenesis. Science 2018;360(6385):204–08. doi: 10.1126/science.aar3799 [published Online First: 2018/04/14] [PubMed: 29650672]
3. Lei W, Ren W, Ohmoto M, et al. Activation of intestinal tuft cell-expressed Sucnr1 triggers type 2 immunity in the mouse small intestine. Proc Natl Acad Sci U S A 2018;115(21):5552–57. doi: 10.1073/pnas.1720758115 [published Online First: 2018/05/08] [PubMed: 29735652]
4. Nadjsombati MS, McGinty JW, Lyons-Cohen MR, et al. Detection of Succinate by Intestinal Tuft Cells Triggers a Type 2 Innate Immune Circuit. Immunity 2018;49(1):33–41 e7. doi: 10.1016/j.immuni.2018.06.016 [published Online First: 2018/07/19] [PubMed: 30021144]
5. Banerjee A, McKinley ET, von Moltke J, et al. Interpreting heterogeneity in intestinal tuft cell structure and function. J Clin Invest 2018;128(5):1711–19. doi: 10.1172/JCI120330 [published Online First: 2018/05/02] [PubMed: 29714721]
6. Howitt MR, Lavoie S, Michaud M, et al. Tuft cells, taste-chemosensory cells, orchestrate parasite type 2 immunity in the gut. Science 2016;351(6279):1329–33. doi: 10.1126/science.aaf1648 [published Online First: 2016/02/06] [PubMed: 26847546]
7. Hogan SP, Seidu L, Blanchard C, et al. Resistin-like molecule beta regulates innate colonic function: barrier integrity and inflammation susceptibility. J Allergy Clin Immunol 2006;118(1):257–68. doi: 10.1016/j.jaci.2006.04.039 [published Online First: 2006/07/04] [PubMed: 16815164]
8. Gerbe F, Sidot E, Smyth DJ, et al. Intestinal epithelial tuft cells initiate type 2 mucosal immunity to helminth parasites. Nature 2016;529(7585):226–30. doi: 10.1038/nature16527 [published Online First: 2016/01/15] [PubMed: 26762460]
9. von Moltke J, Ji M, Liang HE, et al. Tuft-cell-derived IL-25 regulates an intestinal ILC2-epithelial response circuit. Nature 2016;529(7585):221–5. doi: 10.1038/nature16161 [published Online First: 2015/12/18] [PubMed: 26675736]
10. Banerjee A, Herring CA, Chen B, et al. Succinate Produced by Intestinal Microbes Promotes Specification of Tuft Cells to Suppress Ileal Inflammation. Gastroenterology 2020;159(6):2101–15.e5. doi: 10.1053/j.gastro.2020.08.029 [published Online First: 2020/08/24] [PubMed: 32828819]
11. Chandrakesan P, Weygant N, May R, et al. DCLK1 facilitates intestinal tumor growth via enhancing pluripotency and epithelial mesenchymal transition. Oncotarget 2014;5(19):9269–80. doi: 10.18632/oncotarget.2393 [published Online First: 2014/09/12] [PubMed: 25211188]
12. Westphalen CB, Quante M, Wang TC. Functional implication of Dclk1 and Dclk1-expressing cells in cancer. Small GTPases 2017;8(3):164–71. doi: 10.1080/21541248.2016.1208792 [published Online First: 2016/07/28] [PubMed: 27458755]
13. Barker N Adult intestinal stem cells: critical drivers of epithelial homeostasis and regeneration. Nat Rev Mol Cell Biol 2014;15(1):19–33. doi: 10.1038/nrm3721 [published Online First: 2013/12/12] [PubMed: 24326621]
14. Gassler N Paneth cells in intestinal physiology and pathophysiology. World J Gastrointest Pathophysiol 2017;8(4):150–60. doi: 10.4291/wjgp.v8.i4.150 [published Online First: 2017/12/01] [PubMed: 29184701]
15. Clevers H The intestinal crypt, a prototype stem cell compartment. Cell 2013;154(2):274–84. doi: 10.1016/j.cell.2013.07.004 [published Online First: 2013/07/23] [PubMed: 23870119]
16. Yamada K, Sato K, Morishita S, et al. Establishment of a primary culture method for mouse intestinal epithelial cells by organ culture of fetal small intestine. Biosci33 Biotechnol Biochem 2009;73(8):1849–55. doi: 10.1271/bbb.90246 [published Online First: 2009/08/08]
17. Park JH, Kotani T, Konno T, et al. Promotion of Intestinal Epithelial Cell Turnover by Commensal Bacteria: Role of Short-Chain Fatty Acids. PLoS One 2016;11(5):e0156334. doi: 10.1371/journal.pone.0156334 [published Online First: 2016/05/28] [PubMed: 27232601]

18. Hooper LV, Gordon JI. Commensal host-bacterial relationships in the gut. Science 2001;292(5519):1115–8. doi: 10.1126/science.1058709 [published Online First: 2001/05/16] [PubMed: 11352068]
19. Gracz AD, Samsa LA, Fordham MJ, et al. Sox4 Promotes Atoh1-Independent Intestinal Secretory Differentiation Toward Tuft and Enteroendocrine Fates. Gastroenterology 2018;155(5):1508–23 e10. doi: 10.1053/j.gastro.2018.07.023 [published Online First: 2018/07/29] [PubMed: 30055169]
20. Gerbe F, van Es JH, Makrini L, et al. Distinct ATOH1 and Neurog3 requirements define tuft cells as a new secretory cell type in the intestinal epithelium. J Cell Biol 2011;192(5):767–80. doi: 10.1083/jcb.201010127 [published Online First: 2011/03/09] [PubMed: 21383077]
21. Banerjee A, Herring CA, Chen B, et al. Succinate Produced by Intestinal Microbes Promotes Specification of Tuft Cells to Suppress Ileal Inflammation. Gastroenterology 2020;159(6):2101–15 e5. doi: 10.1053/j.gastro.2020.08.029 [published Online First: 2020/08/24] [PubMed: 32828819]
22. Matsumoto I, Ohmoto M, Narukawa M, et al. Skn-1a (Pou2f3) specifies taste receptor cell lineage. Nat Neurosci 2011;14(6):685–7. doi: 10.1038/nn.2820 [published Online First: 2011/05/17] [PubMed: 21572433]
23. Zhang X, Bandyopadhyay S, Araujo LP, et al. Elevating EGFR-MAPK program by a nonconventional Cdc42 enhances intestinal epithelial survival and regeneration. JCI Insight 2020;5(16) doi: 10.1172/jci.insight.135923 [published Online First: 2020/07/21]
24. Tu S, Wu WJ, Wang J, et al. Epidermal growth factor-dependent regulation of Cdc42 is mediated by the Src tyrosine kinase. J Biol Chem 2003;278(49):49293–300. doi: 10.1074/jbc.M307021200 [published Online First: 2003/09/25] [PubMed: 14506284]
25. Wang X-Y, Gan M-X, Li Y, et al. Cdc42 induces EGF receptor protein accumulation and promotes EGF receptor nuclear transport and cellular transformation. FEBS Letters 2015;589(2):255–62. doi: 10.1016/j.febslet.2014.11.049 [PubMed: 25497016]
26. Schlessinger K, Hall A, Tolwinski N. Wnt signaling pathways meet Rho GTPases. Genes Dev 2009;23(3):265–77. doi: 10.1101/gad.1760809 [published Online First: 2009/02/11] [PubMed: 19204114]
27. Melendez J, Liu M, Sampson L, et al. Cdc42 Coordinates Proliferation, Polarity, Migration, and Differentiation of Small Intestinal Epithelial Cells in Mice. Gastroenterology 2013;145(4):808–19. doi: 10.1053/j.gastro.2013.06.021 [PubMed: 23792201]
28. Wang L, Yang L, Debidda M, et al. Cdc42 GTPase-activating protein deficiency promotes genomic instability and premature aging-like phenotypes. Proceedings of the National Academy of Sciences 2007;104(4):1248. doi: 10.1073/pnas.0609149104
29. Szczawinska-Poplonyk A, Ploski R, Bernatowska E, et al. A Novel CDC42 Mutation in an 11-Year Old Child Manifesting as Syndromic Immunodeficiency, Autoinflammation, Hemophagocytic Lymphohistiocytosis, and Malignancy: A Case Report. Frontiers in Immunology 2020;11:318. [PubMed: 32231661]
30. Motokawa M, Watanabe S, Nakatomi A, et al. A hot-spot mutation in CDC42 (p.Tyr64Cys) and novel phenotypes in the third patient with Takenouchi-Kosaki syndrome. Journal of Human Genetics 2018;63(3):387–90. doi: 10.1038/s10038-017-0396-5 [PubMed: 29335451]
31. Bucciol G, Pillay B, Casas-Martin J, et al. Systemic Inflammation and Myelofibrosis in a Patient withTakenouchi-Kosaki Syndrome due to CDC42 Tyr64CysMutation. Journal of Clinical Immunology 2020;40(4):567–70. doi: 10.1007/s10875-020-00742-5 [PubMed: 31953712]
32. Chen F, Ma L, Parrini MC, et al. Cdc42 is required for PIP(2)-induced actin polymerization and early development but not for cell viability. Curr Biol 2000;10(13):758–65. doi: 10.1016/s0960-9822(00)00571-6 [published Online First: 2000/07/19] [PubMed: 10898977]
33. Linder P, Jankowsky E. From unwinding to clamping - the DEAD box RNA helicase family. Nat Rev Mol Cell Biol 2011;12(8):505–16. doi: 10.1038/nrm3154 [PubMed: 21779027]
34. Lee YJ, Wang Q, Rio DC. Coordinate regulation of alternative pre-mRNA splicing events by the human RNA chaperone proteins hnRNPA1 and DDX5. Genes Dev 2018;32(15–16):1060–74. doi: 10.1101/gad.316034.118 [published Online First: 2018/07/26] [PubMed: 30042133]
35. Giraud G, Terrone S, Bourgeois CF. Functions of DEAD box RNA helicases DDX5 and DDX17 in chromatin organization and transcriptional regulation. BMB Rep 2018 [published Online First: 2018/10/09]

36. Endoh H, Maruyama K, Masuhiro Y, et al. Purification and identification of p68 RNA helicase acting as a transcriptional coactivator specific for the activation function 1 of human estrogen receptor alpha. Mol Cell Biol 1999;19(8):5363–72. [PubMed: 10409727]
37. Fuller-Pace FV. The DEAD box proteins DDX5 (p68) and DDX17 (p72): multi-tasking transcriptional regulators. Biochim Biophys Acta 2013;1829(8):756–63. doi: 10.1016/j.bbagrm.2013.03.004 [published Online First: 2013/03/26] [PubMed: 23523990]
38. Jensen ED, Niu L, Caretti G, et al. p68 (Ddx5) interacts with Runx2 and regulates osteoblast differentiation. Journal of cellular biochemistry 2008;103(5):1438–51. doi: 10.1002/jcb.21526 [published Online First: 2007/10/26] [PubMed: 17960593]
39. Abbasi N, Long T, Li Y, et al. DDX5 promotes oncogene C3 and FABP1 expressions and drives intestinal inflammation and tumorigenesis. Life Sci Alliance 2020;3(10) doi: 10.26508/lsa.202000772 [published Online First: 2020/08/21]
40. Causevic M, Hislop RG, Kernohan NM, et al. Overexpression and poly-ubiquitylation of the DEAD-box RNA helicase p68 in colorectal tumours. Oncogene 2001;20(53):7734–43. doi: 10.1038/sj.onc.1204976 [PubMed: 11753651]
41. Lee H, Flaherty P, Ji HP. Systematic genomic identification of colorectal cancer genes delineating advanced from early clinical stage and metastasis. BMC Med Genomics 2013;6:54–54. doi: 10.1186/1755-8794-6-54 [PubMed: 24308539]
42. Cristescu R, Lee J, Nebozhyn M, et al. Molecular analysis of gastric cancer identifies subtypes associated with distinct clinical outcomes. Nature medicine 2015;21(5):449–56. doi: 10.1038/nm.3850 [published Online First: 2015/04/22]
43. Du C, Li D-q, Li N, et al. DDX5 promotes gastric cancer cell proliferation in vitro and in vivo through mTOR signaling pathway. Scientific Reports 2017;7(1):42876. doi: 10.1038/srep42876 [PubMed: 28216662]
44. Ma Z, Feng J, Guo Y, et al. Knockdown of DDX5 Inhibits the Proliferation and Tumorigenesis in Esophageal Cancer. Oncology research 2017;25(6):887–95. doi: 10.3727/096504016×14817158982636 [published Online First: 2017/03/01] [PubMed: 28244855]
45. Nicol SM, Bray SE, Derek Black H, et al. The RNA helicase p68 (DDX5) is selectively required for the induction of p53-dependent p21 expression and cell-cycle arrest after DNA damage. Oncogene 2012 doi: 10.1038/onc.2012.426 [published Online First: 2012/09/19]
46. Grivennikov SI, Wang K, Mucida D, et al. Adenoma-linked barrier defects and microbial products drive IL-23/IL-17-mediated tumour growth. Nature 2012;491(7423):254–8. doi: 10.1038/nature11465 [published Online First: 2012/10/05] [PubMed: 23034650]
47. Miura N, Yamamoto M, Fukutake M, et al. Anti-CD3 induces bi-phasic apoptosis in murine intestinal epithelial cells: possible involvement of the Fas/Fas ligand system in different T cell compartments. International Immunology 2005;17(5):513–22. doi: 10.1093/intimm/dxh231 [PubMed: 15778290]
48. Bankhead P, Loughrey MB, Fernandez JA, et al. QuPath: Open source software for digital pathology image analysis. Sci Rep 2017;7(1):16878. doi: 10.1038/s41598-017-17204-5 [published Online First: 2017/12/06] [PubMed: 29203879]
49. Sano T, Huang W, Hall JA, et al. An IL-23R/IL-22 Circuit Regulates Epithelial Serum Amyloid A to Promote Local Effector Th17 Responses. Cell 2015;163(2):381–93. doi: 10.1016/j.cell.2015.08.061 [PubMed: 26411290]
50. Miyoshi H, Stappenbeck TS. In vitro expansion and genetic modification of gastrointestinal stem cells in spheroid culture. Nature protocols 2013;8(12):2471–82. doi: 10.1038/nprot.2013.153 [published Online First: 11/14] [PubMed: 24232249]
51. McGinty JW, Ting HA, Billipp TE, et al. Tuft-Cell-Derived Leukotrienes Drive Rapid Anti-helminth Immunity in the Small Intestine but Are Dispensable for Anti-protist Immunity. Immunity 2020;52(3):528–41 e7. doi: 10.1016/j.immuni.2020.02.005 [published Online First: 2020/03/12] [PubMed: 32160525]
52. Subramanian A, Tamayo P, Mootha VK, et al. Gene set enrichment analysis: a knowledge-based approach for interpreting genome-wide expression profiles. Proc Natl Acad Sci U S A 2005;102(43):15545–50. doi: 10.1073/pnas.0506580102 [published Online First: 2005/10/04] [PubMed: 16199517]

53. Heinz S, Benner C, Spann N, et al. Simple combinations of lineage-determining transcription factors prime cis-regulatory elements required for macrophage and B cell identities. Mol Cell 2010;38(4):576–89. doi: 10.1016/j.molcel.2010.05.004 [published Online First: 2010/06/02] [PubMed: 20513432]

54. Wood DE, Salzberg SL. Kraken: ultrafast metagenomic sequence classification using exact alignments. Genome Biology 2014;15(3):R46. doi: 10.1186/gb-2014-15-3-r46 [PubMed: 24580807]

55. Peters LA, Perrigoue J, Mortha A, et al. A functional genomics predictive network model identifies regulators of inflammatory bowel disease. Nat Genet 2017;49(10):1437–49. doi: 10.1038/ng.3947 [published Online First: 2017/09/12] [PubMed: 28892060]

56. Vancamelbeke M, Vanuytsel T, Farre R, et al. Genetic and Transcriptomic Bases of Intestinal Epithelial Barrier Dysfunction in Inflammatory Bowel Disease. Inflamm Bowel Dis 2017;23(10):1718–29. doi: 10.1097/MIB.0000000000001246 [published Online First: 2017/09/09] [PubMed: 28885228]

57. Herring CA, Banerjee A, McKinley ET, et al. Unsupervised Trajectory Analysis of Single-Cell RNA-Seq and Imaging Data Reveals Alternative Tuft Cell Origins in the Gut. Cell Syst 2018;6(1):37–51 e9. doi: 10.1016/j.cels.2017.10.012 [published Online First: 2017/11/21] [PubMed: 29153838]

58. Gracz AD, Samsa LA, Fordham MJ, et al. Sox4 Promotes Atoh1-Independent Intestinal Secretory Differentiation Toward Tuft and Enteroendocrine Fates. Gastroenterology 2018;155(5):1508–23.e10. doi: 10.1053/j.gastro.2018.07.023 [published Online First: 2018/07/29] [PubMed: 30055169]

59. Sakamori R, Das S, Yu S, et al. Cdc42 and Rab8a are critical for intestinal stem cell division, survival, and differentiation in mice. J Clin Invest 2012;122(3):1052–65. doi: 10.1172/JCI60282 [published Online First: 2012/02/23] [PubMed: 22354172]

60. McKinley ET, Sui Y, Al-Kofahi Y, et al. Optimized multiplex immunofluorescence single-cell analysis reveals tuft cell heterogeneity. JCI Insight 2017;2(11) doi: 10.1172/jci.insight.93487 [published Online First: 2017/06/02]

What is already known on this subject?

- A subset of intestinal epithelial cells known as tuft cells orchestrates mucosal defense against helminths and parasites, contributes to epithelial repair, and reduces ileal inflammation, but also serves as a viral reservoir and harbors tumor stem cell properties.
- Tuft cell specification requires Rho GTPase Cell Division Cycle 42 (CDC42) and the master transcription factor POU class 2 homeobox 3 (POU2F3). However, little is known about how this pathway is regulated *in vivo*.
- RNA helicase DDX5 promotes tumorigenesis in the small intestine and colon. However, little is known about its role in normal IEC differentiation and function.

What are the new findings?

- In the small intestine, knocking out DDX5 specifically in intestinal epithelial cells results in a dramatic reduction of intestinal tuft cell numbers and exacerbation of ileal inflammation,
- In the colon, knocking out DDX5 specifically in intestinal epithelial cells results in alteration of microbial composition and protection against colonic tumorigenesis.
- Mechanistically, DDX5 binds to and drives the translation of *Cdc42* transcripts to maintain proper CDC42 level in the secretory progenitor cells required for *Pou2f3* expression and tuft cell specification.

What is the foreseeable clinical impact?

- Our findings reveal an epithelial cell intrinsic (DDX5-CDC42-POU2F3) pathway in promoting intestinal tuft cell specification. Modulation of this pathway may have therapeutic potentials for combating ileal inflammation and colonic cancers.

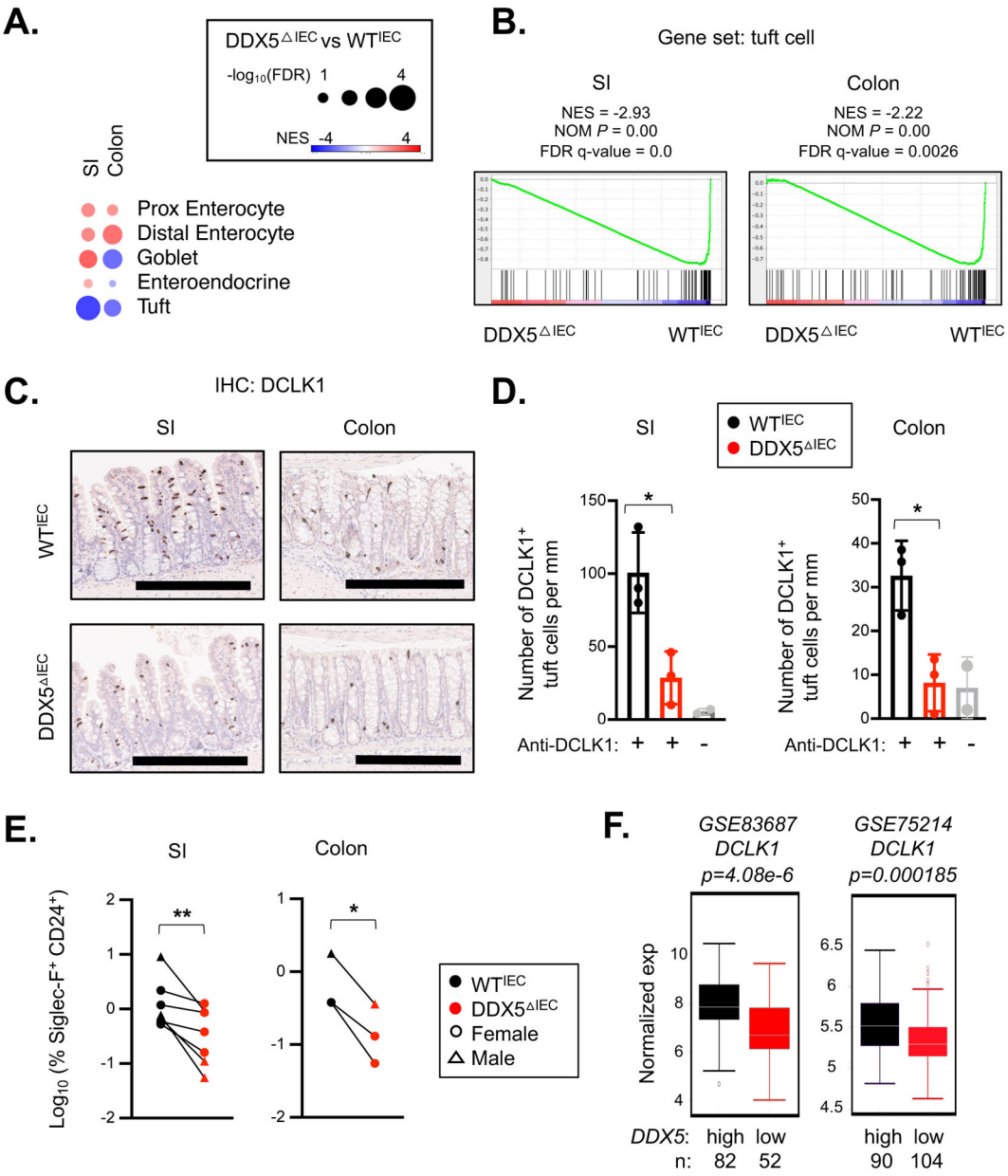

Figure 1. Epithelial DDX5 promotes the tuft cell gene program in the intestine.

A. Heatmap summarizing the GSEA results on the indicated IEC gene subsets in the RNAseq dataset obtained from the ileal (SI) and colonic IECs of two pairs of male WT^{IEC} and $DDX5^{\Delta IEC}$ mice (GSE123881). NES, normalized enrichment score; FDR, false discovery rate.

B. GSEA enrichment plots of the tuft cell gene set in WT^{IEC} and $DDX5^{\Delta IEC}$ ileal (SI) and colonic IECs from A. NES, normalized enrichment score; NOM *P*, normalized nominal *p*-value.

C. Representative images from immunohistochemistry analysis of $DCLK1^{+}$ cells in intestinal sections from female WT^{IEC} and $DDX5^{\Delta IEC}$ mice. Scale bar represents 300μm.

D. DCLK1^{+} tuft cell counts on ileal (SI) and colonic sections from 3 pairs of female WT^{IEC} (black, n=3) and DDX5$^{\Delta IEC}$ (red, n=3) mice analyzed according to the automated workflow described in Supplementary Figure 2A. Mice were fasted overnight to minimize the impact of varying food intake prior to tissue harvest. Each dot represents the result from one mouse. No primary antibody controls are shown in grey. * p<0.05 (unpaired t-test).

E. Summary of flow cytometry results of WT^{IEC} and DDX5$^{\Delta IEC}$ ileal (SI) and colonic epithelium. IECs were defined as live CD4^{-}CD8^{-}Epcam^{+}CD45^{low}. Proportion (%) of IECs in the tuft cell lineage defined as Siglec-F^{+}CD24^{+} are graphed. See Supplementary Figure 3A for gating strategy. Each dot represents the result from one mouse. * p<0.05, ** p<0.01 (paired t-test).

F. Human *DCLK1* expression in colonic biopsies with *DDX5* expression below (low) or above (high) the mean of each respective dataset (GSE83687[55] and GSE75214[56]).

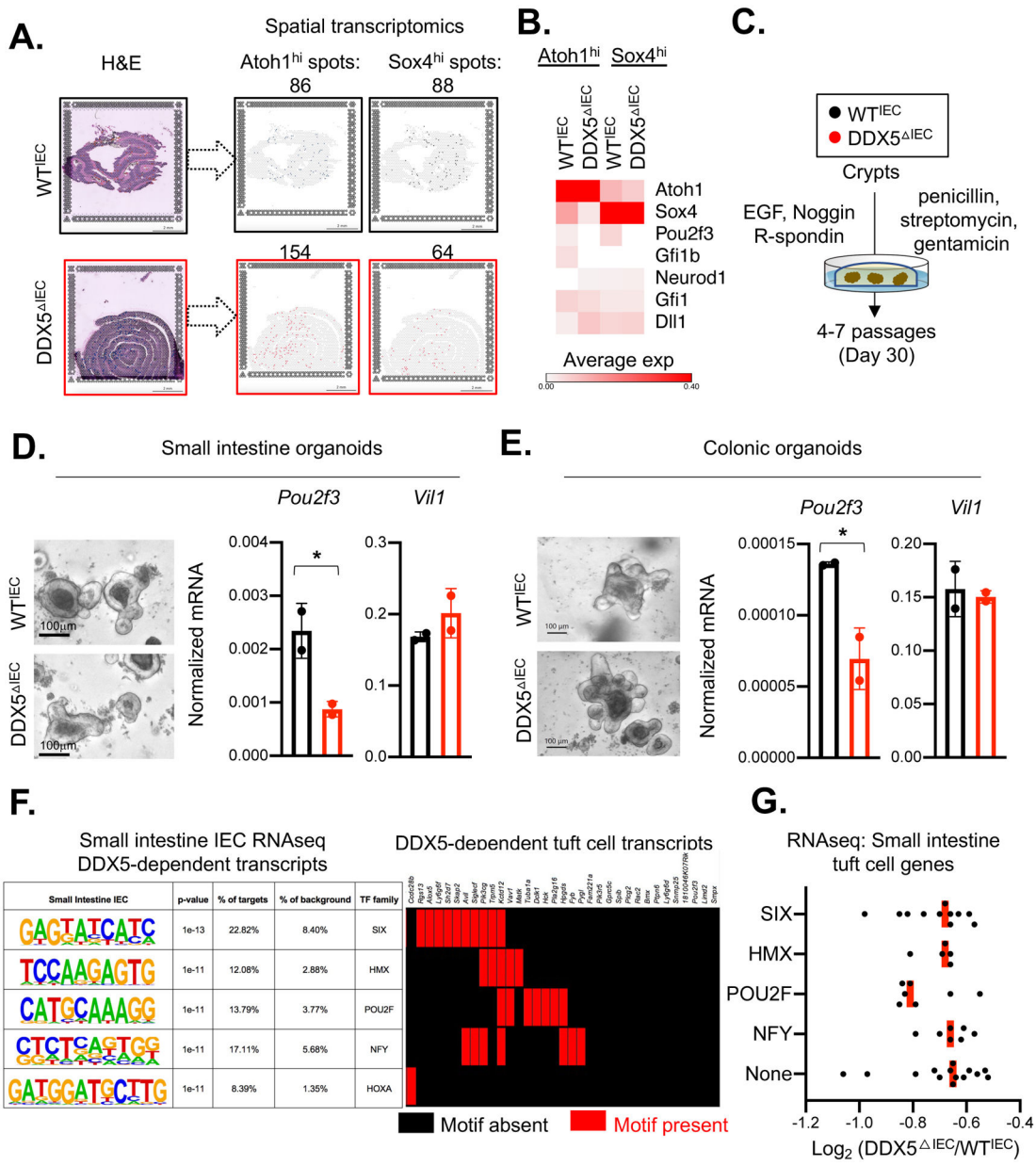

Figure 2. Spatial transcriptomic analysis revealed altered secretory lineage progenitor signature in the DDX5$^{\Delta IEC}$ mice.

A. Left: H&E staining of the small intestinal swiss rolls from one pair of female WT^{IEC} and DDX5$^{\Delta IEC}$ littermates used for the spatial transcriptomic analysis (Visium, 10X Genomic). Right: Loupe browser displaying *Atoh1*^{high} or *Sox4*^{high} spots on each tissue section. Scale bar: 2mm.

B. Heatmap indicating the average expression of IEC lineage-specifying genes in *Atoh1*^{high} or *Sox4*^{high} spots indicated in A.

C. Schematic of establishing intestinal crypt organoid cultures.

D. Left: Representative bright field images of organoids established from small intestinal crypts of WT^{IEC} and DDX5$^{\Delta IEC}$ mice following the protocol outlined in[50]. Scale bar, 100μm. Right: Normalized mRNA expressions of *Pou2f3* and *Vil1* from WT^{IEC} (n=2) and

DDX5$^{\Delta IEC}$ (n=2) small intestinal organoids cultured over 4–7 passages. Each dot represents the result from an independent organoid experiment. Results were averaged from two independent biological experiments. * $p<0.05$ (unpaired *t*-test).

E. Left: Representative bright field images of organoids established from colonic crypts of WT^{IEC} and DDX5$^{\Delta IEC}$ mice following the protocol outlined in[50]. Scale bar, 100μm. Right: Normalized mRNA expressions of *Pou2f3* and *Vil1* from WT^{IEC} and DDX5$^{\Delta IEC}$ colonic organoids cultured over 4–7 passages. Each dot represents the result from an independent organoid experiment. Results were averaged from two independent biological experiments. * $p<0.05$ (unpaired *t*-test).

F. Left: HOMER *de novo* analysis identified the top 5 motifs present at the promoters (defined as −1 kb to +500 bp from the transcription start site) of all ileal IEC DDX5-dependent genes identified in Figure 1A[39]. Promoters from all other IEC expressed genes were used as background. Right: The presence (red) or absence (black) of the motifs indicated on the left at the tuft cell DDX5-dependent gene promoters.

G. Average $\log_2$ fold change of the transcript abundance of tuft cell-expressed genes harboring SIX, HMX, POU2F, NFY motifs, or None of the above motifs at their promoters in ileal IECs from two independent pairs of WT^{IEC} and DDX5$^{\Delta IEC}$ littermates. Each dot represents one gene.

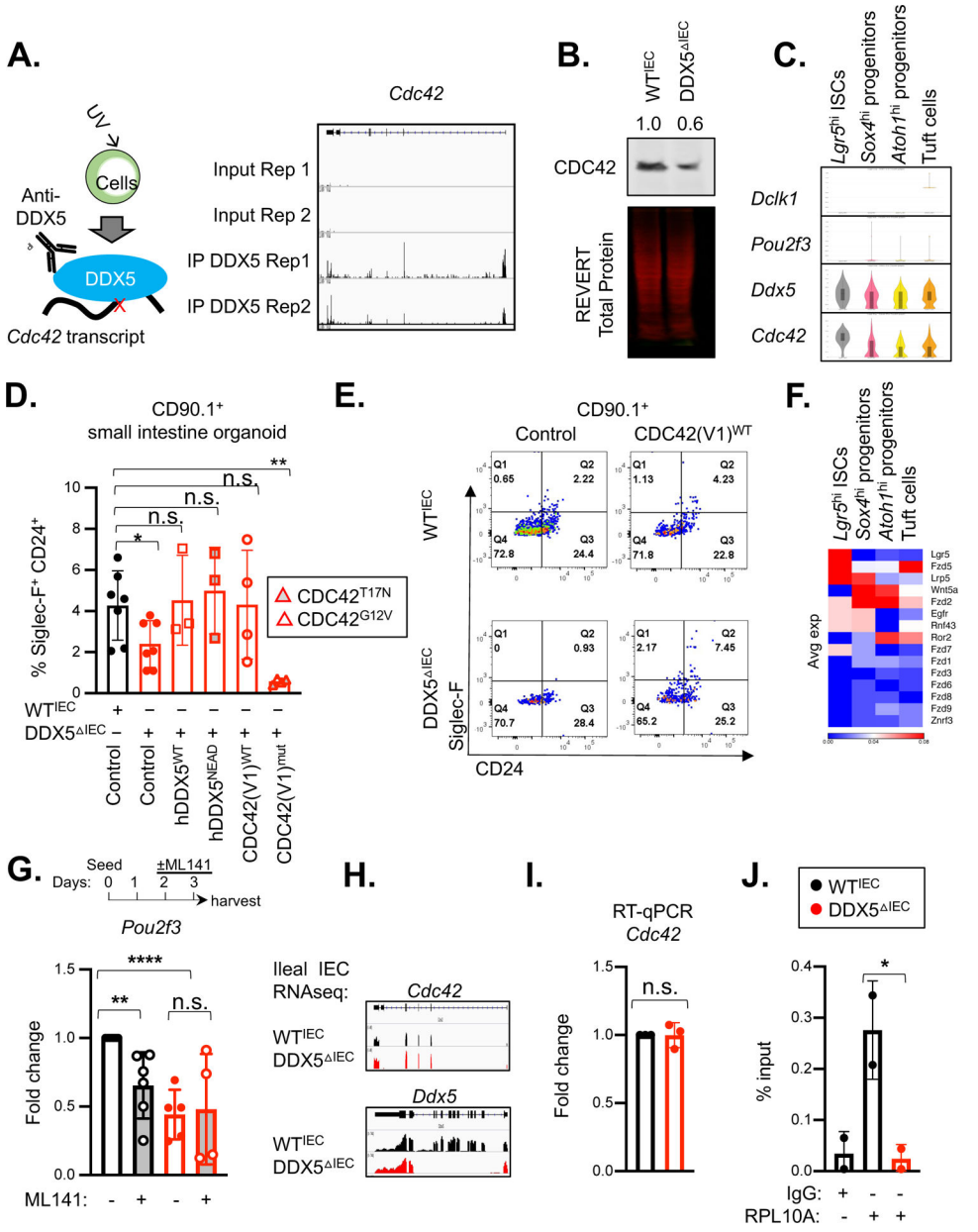

Figure 3. DDX5 regulates *Pou2f3* expression and tuft cell specification by promoting *Cdc42* translation.

A. Left: Schematic representation of the enhanced CLIP (eCLIPseq) experiment. Right: Integrative Genomics Viewer (IGV) browser view of DDX5 eCLIPseq signals at the *Cdc42* loci from two independent experiments.

B. Representative western blot for CDC42 in whole cell lysates of small intestinal IECs from WT^{IEC} and $DDX5^{\Delta IEC}$ mice. Experiments were repeated three times using independent biological samples with similar results.

C. Violin plots displaying expression of *Dclk1*, *Pou2f3*, *Ddx5*, and *Cdc42* in small intestinal stem cells (ISC, $Lgr5^{hi}$), $Atoh1^{hi}$ and $Sox4^{hi}$ secretory lineage progenitors, or tuft cells from the spatial transcriptomics dataset described in Figure 2A.

D. Summary of the % of SiglecF^{+}CD24^{+} tuft cells in WT^{IEC} and DDX5$^{\Delta IEC}$ small intestinal organoids 7 days post-transduction with retrovirus (marked by CD90.1^{+}) carrying the indicated expression vectors. Each dot represents the result from an independent organoid experiment. n.s. not significant, * p<0.05, ** p<0.01 (unpaired t-test).

E. Representative flow cytometry plots from D.

F. Heatmap indicating the average expression of known signaling molecules upstream of CDC42 activation in ISCs, progenitors, and tuft cells from Figure 2A.

G. Fold change of *Pou2f3* mRNA in WT^{IEC} (n=6) or DDX5$^{\Delta IEC}$ (n=5) small intestine organoids cultured in the presence of CDC42 inhibitor ML141 (10μM) for 24 hours relative to WT^{IEC} cells treated with vehicle control (DMSO). Each dot represents the result from one mouse. n.s. not significant, ** p<0.01, **** p<0.001 (unpaired t-test).

H. IGV browser view of WT^{IEC} and DDX5$^{\Delta IEC}$ ileal IEC RNAseq-derived sample reads mapped to the *Ddx5* and *Cdc42* loci (GSE123881).

I. Fold change of ileal *Cdc42* mRNA in DDX5$^{\Delta IEC}$ mice (n=3) relative to values found in WT^{IEC} mice (n=3). Each dot represents the result from one mouse. n.s. not significant (unpaired t-test).

J. Ribosome RPL10A enrichment from *Cdc42* mRNA in small intestinal IECs. Results shown represent the average of two independent experiments. Each dot represents the result from one mouse. * p<0.05 (unpaired t-test).

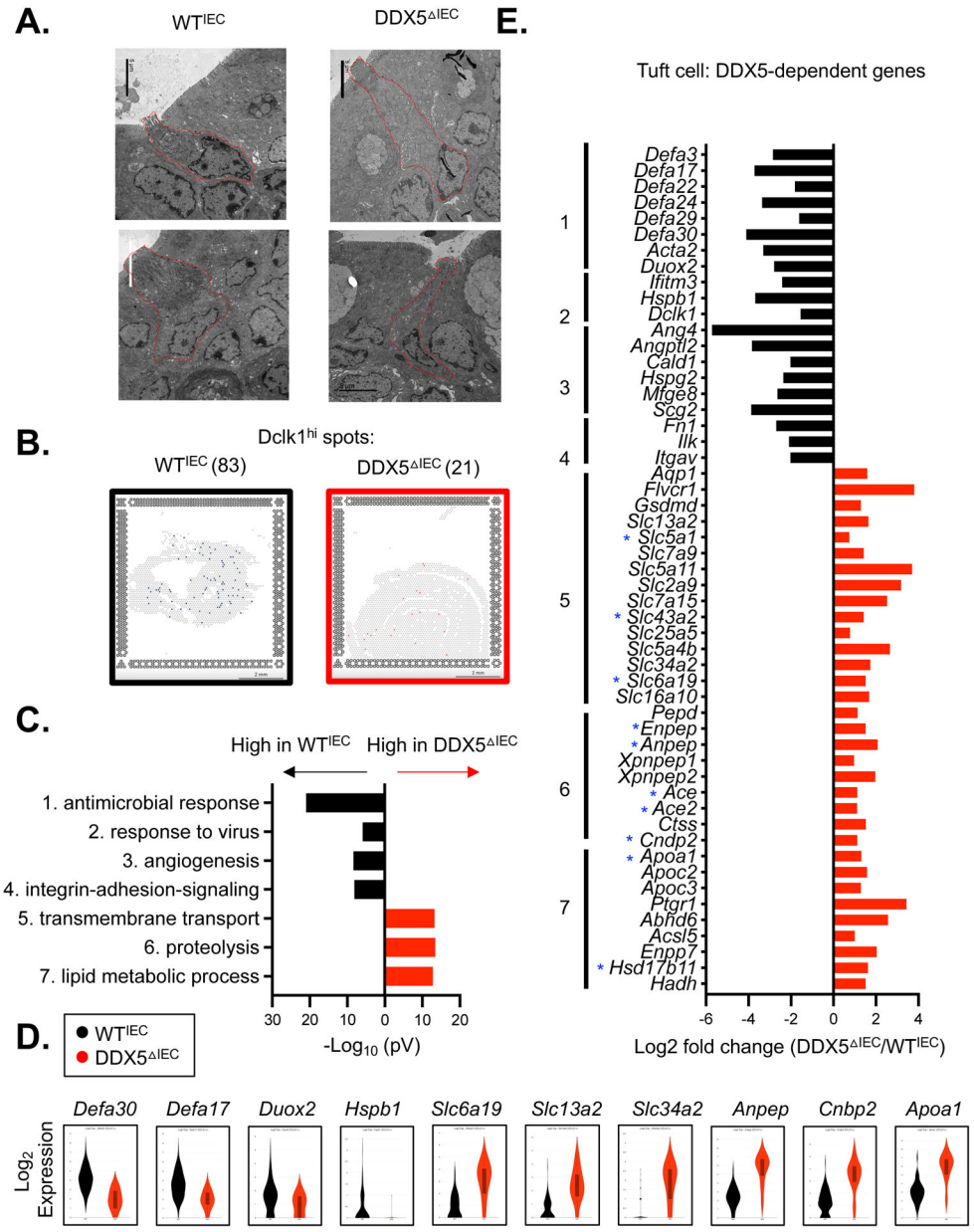

Figure 4. DDX5-dependent tuft cell gene programs in the small intestine.

A. Representative electron microscopy images of small intestinal tuft cells from WT^{IEC} and $DDX5^{\Delta IEC}$ mice. Scale bar: 5μm.

B. Loupe browser screenshots displaying quantified *Dclk1*^{hi} spots on the small intestinal sections from WT^{IEC} and $DDX5^{\Delta IEC}$ mice described in Figure 2A. Scale bar: 2mm.

C. Gene ontology analysis revealed the top 7 pathways downregulated (black) or upregulated (red) in $DDX5^{\Delta IEC}$ *Dclk1*^{hi} cells from B.

D. Violin plots displaying expressions of DDX5-dependent genes—with or without DDX5-associated transcripts—involved in the antimicrobial response (*Defa3* and *Defa17*), viral response (*Duox2* and *Hspb1*), transport (*Slc6a19*), proteolysis (*Anpep* and *Cnbp2*), or lipid metabolism (*Apoa1*) in WT^{IEC} and $DDX5^{\Delta IEC}$ *Dclk1*^{hi} cells from C.

E. Log fold changes ($DDX5^{\Delta IEC}$/ WT^{IEC}) in the expression of tuft cell DDX5-dependent genes participating in pathways identified in C. Small intestinal IEC DDX5-associated transcripts identified in eCLIP analysis are indicated with a blue star (GSE124023).

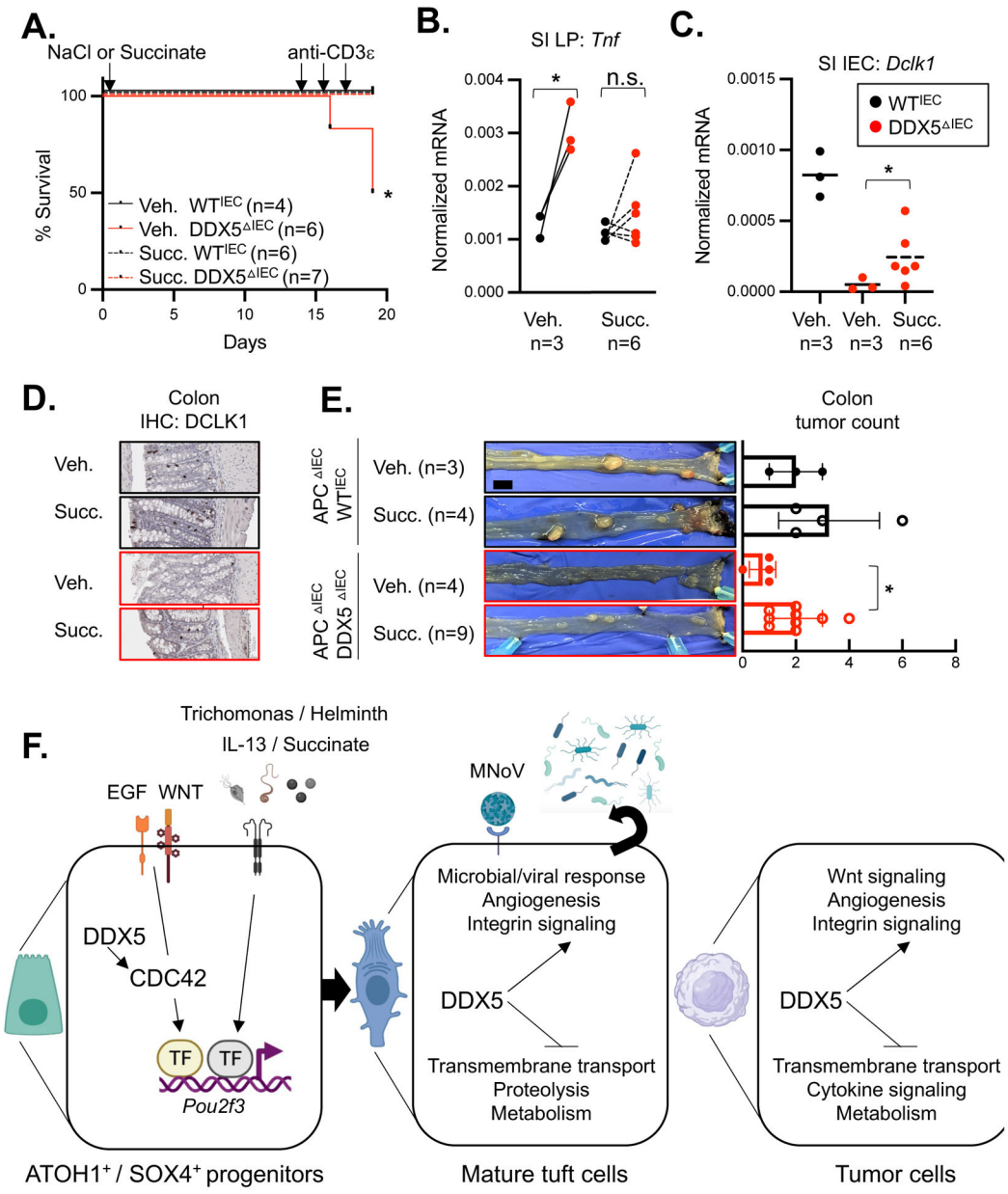

Figure 5. Succinate-induced tuft cell hyperplasia protects DDX5$^{\Delta IEC}$ mice against exacerbated ileitis and restores tumorigenic potential in the DDX5$^{\Delta IEC}$ colon.

A. Survival plot of mice treated with succinate-NaCl (Succ., WT^{IEC}, n=6; DDX5$^{\Delta IEC}$, n=7) or equal molar of NaCl (Veh., WT^{IEC}, n=4; DDX5$^{\Delta IEC}$, n=6) in drinking water for 2 weeks and subsequently challenged by by 15μg of anti-CD3ε per mouse for 5 days. * p<0.05 (Mantel-Cox test).

B. Normalized mRNA expression of *Tnf* in small intestinal lamina propria (LP) mononuclear cells isolated from mice from A on day 19. Each dot represents the result of one mouse. n.s. not significant, * p<0.05 (paired t-test).

C. Normalized mRNA expression of *Dclk1* in the small intestinal IECs isolated from mice from A on day 19. One dot represents the result of one mouse. * p<0.05 (unpaired t-test).

D. Representative images of DCLK1 staining in colon from mice treated with NaCl (Veh.) or succinate-NaCl in drinking water for 30 days. Scale bar represents 100μm.
E. Left: Representative images of colonic tumors from 120 days old $APC^{\Delta IEC}$ $DDX5^{WT}$ and $APC^{\Delta IEC}$ $DDX5^{\Delta IEC}$ mice treated with succinate-NaCl or equal molar of NaCl in drinking water on day 90 for 30 days. Right: Summary of colonic tumor counts from treated $APC^{\Delta IEC}$ $DDX5^{WT}$ and $APC^{\Delta IEC}$ $DDX5^{\Delta IEC}$ mice. Each dot represents the result from one mouse. * $p<0.05$ (unpaired *t*-test). Scale bar represents 1cm.
F. Working model. Left: DDX5-CDC42-POU2f3 axis regulating progenitor commitment toward the tuft cell lineage. Right: DDX5-dependent gene programs in differentiated tuft cells.